3394–3403 *Nucleic Acids Research, 2001, Vol. 29, No. 16*

Effects of base change mutations within an *Escherichia coli* ribosomal RNA leader region on rRNA maturation and ribosome formation

Jan Schäferkordt and Rolf Wagner*

Institut für Physikalische Biologie, Heinrich-Heine-Universität Düsseldorf, Universitätsstraße 1, D-40225 Düsseldorf, Germany

Received April 20, 2001; Revised June 11, 2001; Accepted June 19, 2001

ABSTRACT

The effects of base change mutations in a highly conserved sequence (boxC) within the leader of bacterial ribosomal RNAs (rRNAs) was studied. The boxC sequence preceding the 16S rRNA structural gene constitutes part of the RNase III processing site, one of the first cleavage sites on the pathway to mature 16S rRNA. Moreover, rRNA leader sequences facilitate correct 16S rRNA folding, thereby assisting ribosomal subunit formation. Mutations in boxC cause cold sensitivity and result in 16S rRNA and 30S subunit deficiency. Strains in which all rRNA operons are replaced by mutant transcription units are viable. Thermodynamic studies by temperature gradient gel electrophoresis reveal that mutant transcripts have a different, less ordered structure. In addition, RNA secondary structure differences between mutant and wild-type transcripts were determined by chemical and enzymatic probing. Differences are found in the leader RNA sequence itself but also in structurally important regions of the mature 16S rRNA. A minor fraction of the rRNA transcripts from mutant operons is not processed by RNase III, resulting in a significantly extended precursor half-life compared to the wild-type. The boxC mutations also give rise to a new aberrant degradation product of 16S rRNA. This intermediate cannot be detected in strains lacking RNase III. Together the results indicate that the boxC sequence, although important for RNase III processing, is likely to serve additional functions by facilitating correct formation of the mature 16S rRNA structure. They also suggest that quality control steps are acting during ribosome biogenesis.

INTRODUCTION

Today, based on the efforts of many laboratories over the past decades, we have detailed knowledge of the three-dimensional structure of bacterial ribosomes at high resolution (1–7). Much less is known, however, about the complex processes of synthesis of ribosomal constituents and their cooperative assembly into functional particles. Ribosomes are essential components for cell growth. Hence, their biosynthesis is tightly coupled to cell demand and their number is precisely adjusted to environmental changes (8,9). Within the complex network of highly regulated constituents the ribosomal RNAs (rRNAs) are the key molecules for ribosome formation. Thus, there is considerable interest in understanding the regulation of rRNA synthesis and the complex steps of maturation and assembly which finally lead to functional ribosomes. In *Escherichia coli* rRNAs are encoded by seven individual transcription units of very similar organisation (10). Transcription yields long precursor molecules where the structural sequences for 16S, 23S and 5S rRNAs and one or several tRNAs are flanked by extra sequences termed leader, spacer or trailer regions. From the continuous primary transcripts the mature rRNAs are formed by a complex series of endonucleolytic processing steps involving a number of specific processing nucleases (11,12). A detailed understanding of the maturation steps is hampered by the fact that processing takes place concomitant with transcription and assembly of ribosomal proteins. The situation can be described by a very complex scenario where rRNA transcription, folding into higher order structure, endonucleolytic cleavage reactions and protein assembly occur simultaneously in a cascade of concerted reactions. Most of the steps are interdependent and highly cooperative. Recent findings have shown that the rRNA leader and spacer sequences are important contributors which actively participate in the maturation process. By forming transient interactions with the mature transcripts, leader sequences have been shown to facilitate rRNA folding and subunit assembly in a chaperone-like way (13–19).

In this study we have analysed the effects of base change mutations within a conserved leader RNA element termed boxC. This sequence is known to form part of the RNase III processing site which is cleaved in one of the first processing steps shortly after transcription of the 16S rRNA has been completed (12). The boxC sequence has also been considered to be part of the *nut*-like elements, which, together with the boxA and boxB sequences, have been suggested to be involved in transcription antitermination (20). Moreover, by analogy with the function of certain eukaryotic snoRNAs, it was proposed that boxC sequences might directly participate in

*To whom correspondence should be addressed. Tel: +49 211 811 4928; Fax: +49 211 811 5167; Email: r.wagner@mail.rz.uni-duesseldorf.de

facilitating the higher order structure of the 16S rRNA by formation of an obligate structural intermediate. This structure then facilitates conversion to the universally conserved central pseudoknot found in the small ribosomal subunits of all living organisms (21).

We show here that base changes in the boxC region of a plasmid encoded rRNA operon confer a cold-sensitive phenotype to cells that harbour the mutations. Effects of the mutations on the thermodynamic stabilities and three-dimensional structures of the rRNA transcripts were characterised *in vitro* employing chemical and enzymatic probing and temperature gradient gel electrophoresis. These studies demonstrate clear differences not only in the conformation of the leader transcript, but also in regions of the 16S rRNA important for correct folding. We have furthermore analysed the fate of rRNA transcripts derived from mutant operons *in vivo*. Our results demonstrate that boxC mutations affect the processing pathway and also the lifetime of correctly processed 16S rRNA. From the results we conclude that the cold-sensitive phenotype of boxC mutants cannot solely be explained by defective RNase III processing, but very likely involves misfolding of the 16S rRNA mediated by base change-dependent structural distortion of the leader RNA.

MATERIALS AND METHODS

Bacterial strains

Escherichia coli strains HB101 (22) CSR603 (23), BL107 (24), ABL1 (25) and TA554 (26) were used. Strain TA554, with all chromosomal rRNA operons inactivated, was a kind gift of C. Squires (Tufts University School of Medicine, Boston, MA).

Plasmids

Plasmids pBR322, pKK3535, pT0, pT11 and pSTL-T0 have been described previously (27–30). Plasmids pC1, pC2 and pC3 are derivatives of pT0 with base transitions in the boxC region (Eberle, unpublished results). The spectinomycin-resistant derivatives pT0-Spec, pC1-Spec, pC2-Spec and pC3-Spec were obtained by cloning the 1780 bp *Xho*I–*Xba*I fragment from pSTL-T0 into the corresponding position of pT0, pC1, pC2 and pC3. For *in vitro* transcription with T7 RNA polymerase the vectors pIKT0 and pIKC3 were constructed from pWB (16) with the corresponding rRNA sequences cloned under control of the T7 promoter. Standard methods for DNA manipulation were used throughout (31).

Temperature gradient gel electrophoresis

Differences in the higher order structure of wild-type and mutant RNA molecules were determined by comparison of their electrophoretic mobilities on 7.5% (w/v) polyacrylamide gels with a linear temperature gradient between 10 and 50°C. The standard separation procedure (32) was followed as recently published (15). Prior to structural analysis, RNA transcripts were routinely subjected to a denaturation–renaturation step by heating to 70°C for 1 min in 20 mM Na cacodylate, pH 7.2, 100 mM KCl, 5 mM $MgCl_2$ and 1 mM EDTA, followed by slow cooling to 10°C. Radiolabelled wild-type and unlabelled mutant transcripts were mixed prior to separation. The gel was silver stained and autoradiographed. Both figures were superimposed for analysis.

Structural probing

Limited enzymatic digestions with RNase T1, nuclease S1 and cobra venom enzyme CVE, as well as the chemical modification reactions with kethoxal, DMS and DEPC, were performed at <20°C as described (33,34). The sites of cleavage or modification were identified by primer extension analysis employing oligonucleotides complementary to selected rRNA sequences (35).

Maxicell labelling of plasmid encoded rRNA transcripts

Specific labelling of plasmid encoded RNA was achieved after transforming the maxicell strain CSR603 with plasmids containing wild-type or mutant rRNA operons. The labelling procedure and RNA preparation were performed as described previously (36,37). RNA products were separated on composite acrylamide (3% w/v)–agarose (0.5% w/v) gels. Radiolabelled bands were visualised by autoradiography and quantified according to densitometric evaluation of band intensities.

Determination of RNA half-lives *in vivo*

Rifampicin (final concentration 500 µg/ml) was added to exponentially growing cells when they reached an optical density of ~0.5 OD_{600}. Aliquots of the culture were withdrawn, immediately before and at 20 s time intervals after rifampicin addition. Total RNA was extracted by the hot phenol method (38) and concentrated by ethanol precipitation. The RNA concentration was determined spectrophotometrically and aliquots were subjected to a primer extension analysis (39).

Northern analysis of RNA

Aliquots of 10 µg total RNA extracted after rifampicin addition were separated on 1.2% agarose–6% formaldehyde (w/v) denaturing gels and transferred to a Hybond N membrane (Amersham) by capillary transfer. RNA was UV cross-linked (Stratalinker, 120 mJ) and hybridised with different ^{32}P-labelled oligonucleotide probes (~3×10^6 c.p.m.). Following the washing procedure signals were detected by autoradiography.

Nuclease protection experiments

The 3′-end of processing intermediates was determined by S1 nuclease protection. DNA fragments of the 16S rRNA gene (probe 1, positions 838–945, and probe 2, positions 838–1053) were annealed to total RNA extracts and subjected to S1 hydrolysis. Positions of S1 cleavage were then identified by primer extension employing Klenow DNA polymerase and a 5′-labelled primer oligonucleotide. The exact 3′-ends were identified by a sequencing reaction run in parallel.

Analysis of rRNAs from different cellular ribosomal fractions

Ribosomes were isolated from wild-type and mutant cells grown to mid log phase and separated on sucrose gradients exactly as described (40). After centrifugation the A_{260} was recorded using a UV monitor. The resulting peaks were quantitatively evaluated by integration. To isolate polysomes the method of Godson and Sinsheimer (41) was followed. Cells

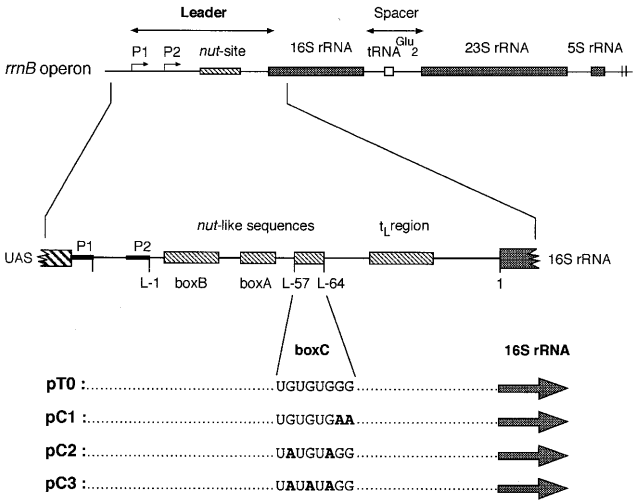

Figure 1. Schematic diagram of the *E.coli rrnB* operon with the leader region extended. Leader and spacer regions are indicated by double-headed arrows. *nut*-like sequences, boxB (positions L-3–L-27), boxA (positions L-30–L-39) and boxC (positions L-57–L-64) as well as the t_L region are marked. UAS denotes the upstream activating sequence. Numbers with the capital letter L indicate sequence positions of the leader relative to the transcription start at promoter P2. The 5′-end of the 16S rRNA sequence is denoted by the number 1. Transition mutations within the boxC region of plasmids pC1–pC3 are indicated in bold.

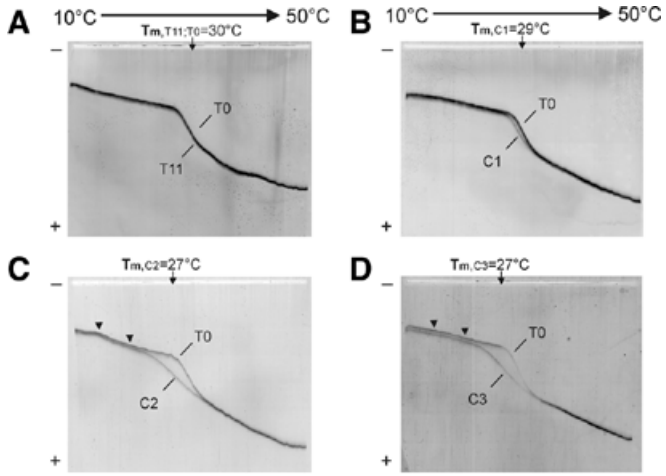

Figure 2. Structural analysis of mutant transcripts by temperature gradient gel electrophoresis. A mixture of radiolabelled wild-type and non-labelled mutant transcripts were separated in each case. Wild-type (T0) and mutant (T11, C1, C2 and C3) transcripts are indicated. The direction of the temperature gradient (10–50°C) is indicated by an arrow. T_m values are marked at the top. Arrowheads denote mobility differences at low temperature for C2 and C3 derived transcripts.

were grown to mid log phase, cooled rapidly and the lysate was separated on 15–30% (w/v) sucrose gradients. Peak fractions containing isolated subunits, 70S ribosomes and polysomes were collected according to the absorption profile and the rRNA isolated from these fractions as described (13). For determination of the relative amounts of chromosome (wild-type) versus plasmid encoded (mutant) rRNA we took advantage of strains which carry the spectinomycin resistance marker (C→U change at position 1192 of 16S rRNA). The proportion of C→U in the rRNA samples, corresponding to the proportion of chromosome to plasmid encoded rRNA, was then determined by primer extension reaction (14,42).

RESULTS AND DISCUSSION

Base changes in the leader boxC sequence cause a cold-sensitive growth phenotype

A series of G→A transition mutations in the leader region of the plasmid encoded *E.coli rrnB* operon (pKK3535; 28) have been constructed by bisulfite mutagenesis (Eberle, unpublished results; 29). DNA fragments containing base changes in the leader boxC were subcloned and it was verified by sequencing that mutations were limited to the boxC region. Three mutant plasmids were selected for further investigations (pC1, pC2 and pC3, see Materials and Methods). Each plasmid harboured a different set of base change mutations within the leader boxC sequence of a functional rRNA operon. The altered sequence positions together with the wild-type sequence and their location within the rRNA leader are presented in Figure 1. Transformation of *E.coli* cells with each of the mutant plasmids pC1, pC2 and pC3 resulted in growth reduction of transformed cells. The observed phenotype is clearly cold sensitive. Doubling times of HB101 cells harbouring different boxC mutations have been determined at decreasing temperatures (standard deviation ≤ 3 min). At high temperatures (42°C) cells transformed with the wild-type or the mutant plasmids had about the same growth rates ($\mu \approx 1.1$). At 37°C only HB101/pC1 grows as fast as the wild-type strain ($\mu \approx 1.0$), while HB101/pC2 and HB101/pC3 already had notably reduced growth rates ($\mu_{pC2} = 0.9$; $\mu_{pC3} = 0.8$). At low temperatures (30°C) growth reduction of the transformants became more dramatic ($\mu_{wild\text{-}type} = 0.8$; $\mu_{pC1} = 0.6$; $\mu_{pC2} = 0.5$; $\mu_{pC3} = 0.4$). It should also be noted that the resulting phenotype was increasingly severe for the different mutations in the order pC1 < pC2 < pC3. Since we could not detect any significant differences in the plasmid copy numbers of pC1, pC2 and pC3 transformants it must be concluded that the differential effects on growth rates are not due to variations in the gene dosage, but rather result from the individual boxC base changes (data not shown).

BoxC mutations cause differences in the thermodynamic stabilities of the corresponding transcripts

From previous studies we knew that local base changes in the rRNA leader could give rise to distant structural alterations within the rRNA transcript. To analyse putative mutation-dependent differences in the conformation or thermodynamic stability of leader RNA transcripts we took advantage of the temperature gradient gel electrophoresis (TGGE) technique (32). To this end wild-type (T0) and mutant leader RNAs (C1, C2 and C3) including the first 84 nt of the 16S rRNA were transcribed and, after a denaturation–renaturation step, the radiolabelled wild-type RNA was mixed with each of the non-labelled mutant transcripts. The mixtures were separated on 7.5% native polyacrylamide gels with a continuous temperature gradient (10–50°C). The results presented in Figure 2, where stained gels have been superimposed on the corresponding autoradiograms, reveal significant structural differences for wild-type and mutant boxC leader RNAs. The electrophoresis

patterns differ in three aspects. First, the transition temperature for the major unfolding step, at ~30°C for the wild-type, is shifted to lower temperatures (~27°C) by the mutations (Fig. 2B–D). Second, the high cooperativity of this transition, seen for the wild-type transcript, is lost by the mutations. This loss in cooperativity is more pronounced for transcripts obtained from plasmids giving rise to a more drastic cold sensitivity in the order pC1, pC2, pC3 (Fig. 2B–D). Finally, the mutations in pC2 and pC3 result in structural differences in the corresponding transcripts which are visible by their altered mobility at low temperatures [see the double bands of wild-type (T0) and mutant RNAs (pC2, pC3) in the low temperature region of the gels in Fig. 2C and D]. One has to conclude from this observation that base changes in the boxC region cause folding of the transcripts into slightly different conformations. Hence, the structures of these transcripts differ from the wild-type at low temperature.

In Figure 2A a reference transcript (T11) with base changes in a leader region termed t_L, downstream from boxC, and the wild-type T0 are compared. It should be noted that in this experiment we could not observe a structural difference between 10 and 15°C shown for these two transcripts in a previous investigation (15). While in the former experiment only leader transcripts of 173 nt were analysed, the transcripts employed in this study were longer (257 nt) and contained the first 84 nt of the flanking 16S rRNA.

In summary, the results above show that G→A transitions within the boxC sequence region have a major effect on the structure and stability of leader rRNA transcripts including the first 84 nt of the 16S rRNA. Since the base changes reduce the melting temperature of the transcripts it is reasonable to assume that they cause a less well-ordered structure of lower thermal stability. Moreover, the gradual loss in cooperativity of the melting transitions between 30 and 27°C and the generally faster mobilities of pC2 and pC3 transcripts at low temperature can be taken as an indication of increasingly less regular and less rigid structures if the wild-type RNA is compared with pC1, pC2 or pC3 derived transcripts, respectively. Finally, the degree of structural deviation of the mutant transcripts from the wild-type corresponds with the degree of cold sensitivity caused by the different mutations.

Base changes in boxC cause structural alterations in the leader and 16S rRNA

To determine where exactly the conformational differences induced by leader mutations occur we subjected wild-type and pC3 mutant transcripts to a structural probing analysis. The analysis was performed with transcripts of different length, either containing the leader plus the complete 16S rRNA or a truncated transcript (leader plus the first 84 nt of the 16S rRNA). We employed the structure-specific chemical reagents dimethylsulphate (DMS), which identifies accessible N1-A and N3-C positions, diethylpyrocarbonate (DEPC), which carbethoxylates N7-A, and kethoxal, reacting with N1-G and N2-G if single stranded. Moreover, single- and double-stranded RNA regions were characterised by limited enzymatic hydrolysis with S1 nuclease, RNase T1 and the double strand-specific enzyme CVE (33,43). The sites of modification or cleavage were visualised by primer extension analysis (33,35). To avoid structural heterogeneity during analysis the transcripts were routinely renatured before probing and the modification and cleavage reactions were performed at 20°C or below, where none of the transcripts showed a noticeable melting transition. Results from primer extension analysis are exemplified in Figure 3. (A summary of the data is available as Supplementary Material at NAR Online.) Positions with different accessibilities between wild-type and boxC mutant transcripts are indicated in the secondary structural maps presented in Figure 4. A model of the leader structure according to recent investigations (15) is shown in Figure 4A, while Figure 4B depicts a section of the 16S rRNA secondary structure comprising the 5′-, part of the central and the 3′-domain.

Within the secondary structure of the leader the following changes caused by boxC mutations are apparent. Positions L-C32 and L-U33 within the *nut*-like boxA element are no longer accessible to CVE in the C3 mutant. The nucleotides flanking the boxA sequence (L-U45, L-U47 and L-C48), normally single-stranded in the wild-type, are now CVE reactive, indicating some kind of higher order structure. Positions L-U55–L-U57, upstream of boxC, show enhanced CVE reactivity in the C3 mutant. BoxC positions L-58–L-62, which have been the targets of mutation, are not structurally altered. A notable difference is apparent, however, 3′ to boxC at position L-G63, which becomes highly accessible to kethoxal in the C3 mutant. Changes are also observed for positions L-C143 and L-U149, which are less reactive to CVE in the mutant transcript (Fig. 4A). Structural changes are not limited to the leader but can also be found in the flanking 5′-domain of 16S rRNA. As shown in Figure 4B, positions U12/24 are less reactive to CVE in the mutant and C43 is reactive to S1 and T1 in the wild-type only. Most interestingly, changes are also found more distant from the 5′-domain, namely in the central part of the 16S rRNA and close to the universally conserved pseudoknot, which does not interact directly with the leader. U813, C862, A892 and A906 show enhanced cleavage by CVE in the boxC mutant, suggesting that they are probably involved in additional tertiary interactions.

In summary, the results indicate that boxC mutations not only cause subtle structural rearrangements in the leader itself but also extend their effect into sequence elements of the mature 16S rRNA molecule. Hence, the higher order structure of 16S rRNA transcripts with base changes in the leader boxC is different in the 5′-domain and also in the central part of the molecule close to the universal pseudoknot.

Differential accessibilities of full-length and truncated 16S rRNA transcripts indicate structural reorientations and the occurrence of transient structures during synthesis

Comparison of the chemical and enzymatic probing data for truncated (leader plus the first 84 nt of 16S rRNA) and full-length rRNA transcripts (leader plus complete 16S rRNA) revealed a number of accessibility changes for the different structural probes. The reactivity changes indicate a dynamic folding pathway where sequences of the leader transiently participate in the structure of the 5′-domain of 16S rRNA before the complete 16S sequence is available. Within the leader structure pronounced differences are found in the 3′-stem structure (t_L region) and close to the site where the leader merges into the 5′-end of the 16S rRNA sequence. For instance, in the full-length transcript, as opposed to the truncated RNA, the sequence region L-G144–L-G147 is highly

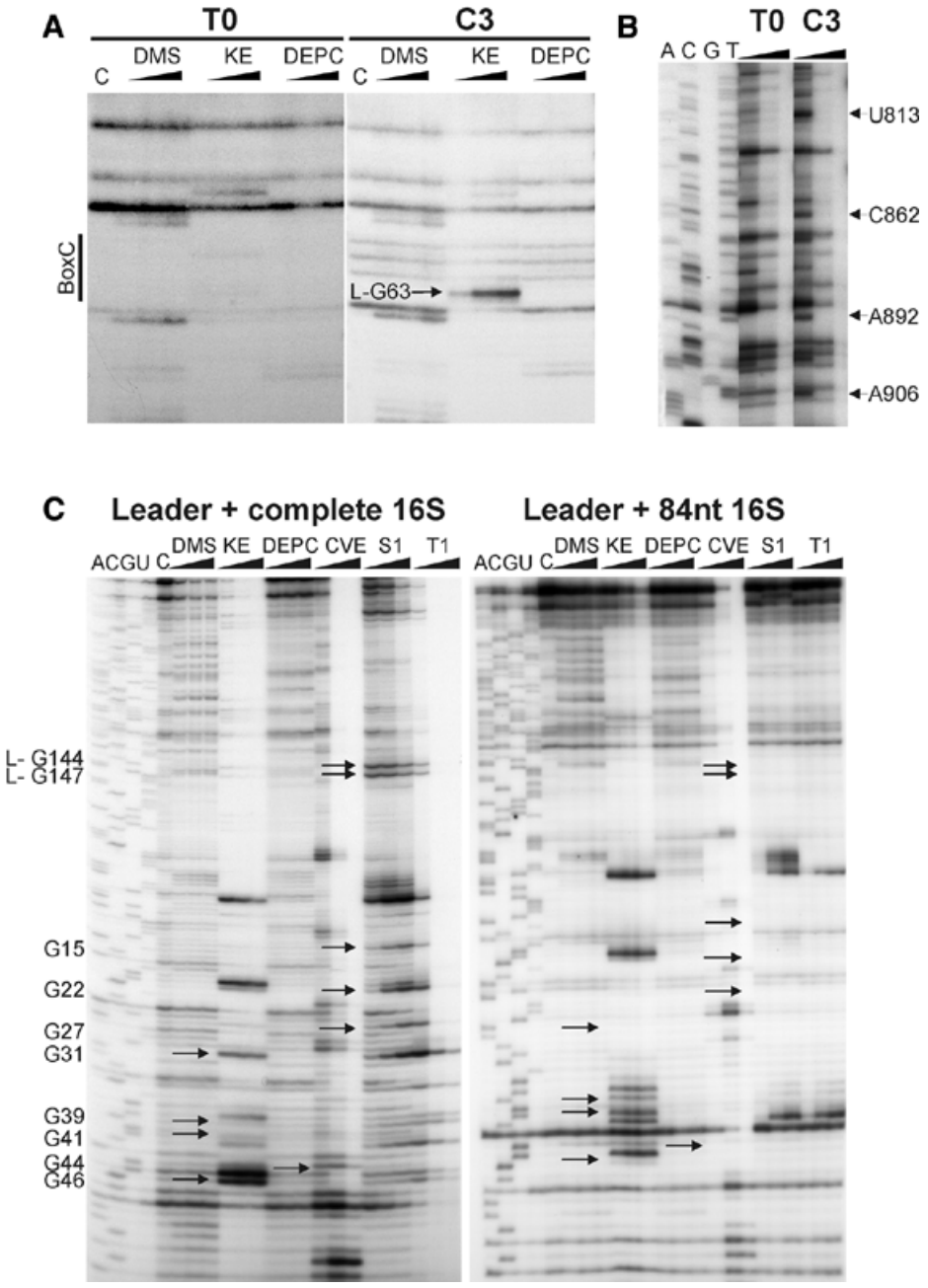

Figure 3. Primer extension after structural probing. The chemical probes used, dimethylsulfate (DMS), kethoxal (KE) and diethylpyrocarbonate (DEPC), and the structure-specific nucleases (S1, T1 and CVE) are indicated at the top of the lanes. A wedge indicates increasing amounts of the respective probe. Sequence positions, according to chain termination sequencing reactions (A, C, G and U), are indicated in the margin. A non-modified control sample (C) was separated in parallel. Arrows highlight structural differences.

accessible to single strand-specific probes (S1 and T1). Within the 5′-domain of 16S rRNA the following changes are observed. The 5′-end (helices 1 and 2, see Fig. 4B for orientation), in line with its involvement in long-range interactions, is folded differently (e.g. positions G15 and G22). Further differences are found for helix 3 (G27 and G31 are more reactive towards single strand-specific probes in the long transcript) and helix 4 (G39 and G41 are not kethoxal reactive in the full-length transcript but G46 shows enhanced kethoxal reactivity). Moreover, several positions within helix 5 and at the 5′-end of helix 6 show altered accessibilities in both transcripts. The observed changes in accessibility suggest a structural reorientation of the 16S rRNA during synthesis. The findings are consistent with the assumption that parts of the leader are involved in folding of the early 16S rRNA sequence. These early structures are metastable and of transient nature. At some point during synthesis a reorientation has to occur and elements of the leader must be withdrawn from the structure to

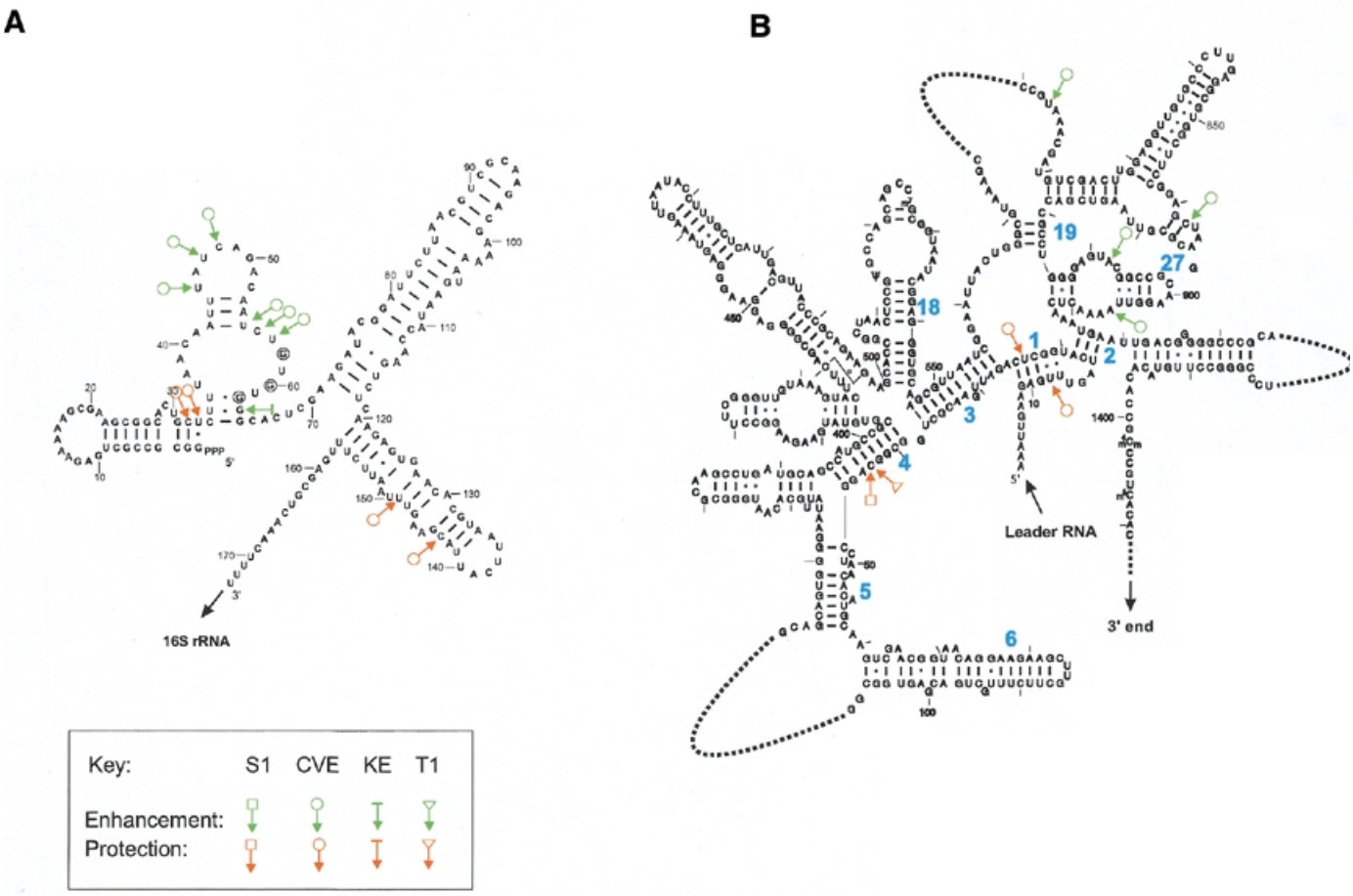

Figure 4. Localisation of structural differences between wild-type and mutant boxC transcripts. (**A**) Schematic arrangement of the secondary structure of the *rrnB* leader RNA (15). Arrows indicate nucleotide positions with altered accessibilities caused by boxC mutations. The different structural probes are shown in colour as given in the key. (**B**) Schematic arrangement of part of the 16S rRNA secondary structure. Helix numbers (according to 44) are depicted in blue. Changes in accessibilities due to boxC mutations are indicated by coloured arrows as given in the key.

enable formation of a helical stem which is recognised by RNase III. Formation of this stem does not occur before the complete 16S rRNA sequence, including the 3′-flanking spacer region, has been transcribed.

Effects of boxC mutations *in vivo*: processing analysis and determination of rRNA and ribosomal stoichiometries

Due to the background of chromosomal rRNA operons, effects resulting from plasmid encoded boxC mutations are difficult to analyse independently. This problem was solved, however, by selective labelling of plasmid encoded RNA transcripts using the maxicell labelling procedure (36,40). Plasmids pC1, pC2 and pC3 carrying the boxC mutations were transformed in the maxicell strain CSR603. After UV-irradiation only transcription from the chromosome is shut-off while plasmid encoded transcripts can be selectively labelled in the presence of [^{32}P]orthophosphate. Ribosomal RNAs were extracted from such cells after the labelling step. Plasmid encoded rRNAs can be visualised separately by comparison of autoradiograms with the staining patterns after gel electrophoretic separation of transcription products. Figure 5 shows an example where RNA extracted from boxC mutant strains had been separated next to a number of rRNA extracts from control transformants. The same gel is shown after staining (Fig. 5A) and autoradiography

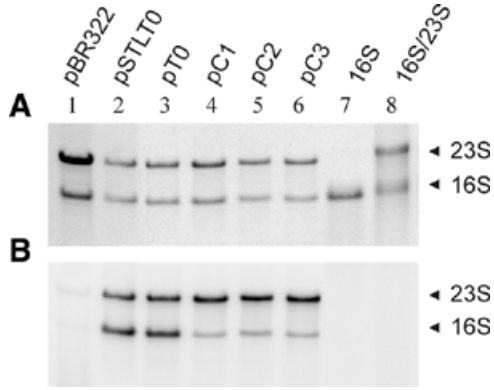

Figure 5. Analysis of rRNA from maxicells. Total RNA isolated after maxicell labelling of strains, transformed with the plasmids indicated, were stained (**A**) and autoradiographed (**B**) after gel separation. The position of mature 16S and 23S rRNAs are indicated. In lanes 7 and 8 marker RNAs were run in parallel. The control pBR322 does not contain extra rRNA operons.

(Fig. 5B), respectively. Comparison with the wild-type rRNAs derived from the chromosome revealed that all the plasmid derived transcripts are correctly processed and rRNAs of the expected size are produced from the plasmid operons with or

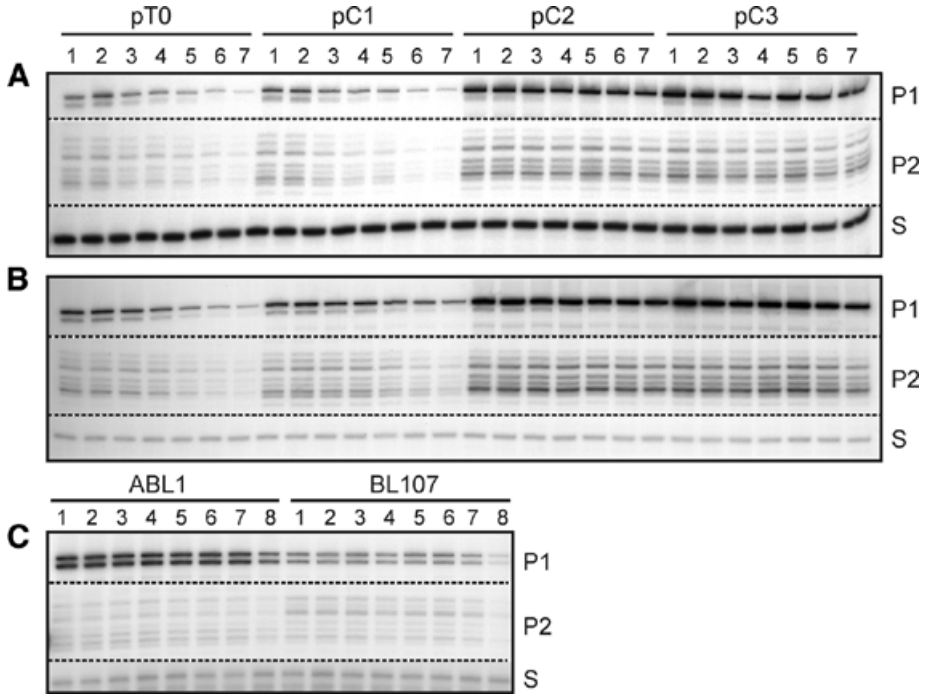

Figure 6. Stability of mutant rRNA transcripts *in vivo*. RNA was isolated after rifampicin addition and analysed by primer extension. (**A** and **B**) RNA from transformed HB101 cells at 37 and 30°C, respectively. The corresponding plasmids are indicated at the top. Products derived from rRNA promoters P1 and P2 are shown. S, an external standard. Numbers indicate time in seconds after rifampicin addition (lanes 1–8: 0, 20, 40, 60, 80, 150, 300 and 900 s). (**C**) Analysis of RNA from the plasmid-free RNase III$^-$ strains ABL1 and BL107.

without boxC mutations. However, comparison of the 23S to 16S rRNA ratios reveals notable differences in rRNA stoichiometry between strains harbouring plasmid encoded rRNA operons with boxC mutations and wild-type rRNA operons or no rRNA operons at all. The normal 16S:23S rRNA ratio of 1:1 is dramatically under-represented (50–75%) in the boxC mutants. The degree of under-representation is very similar for pC1, pC2 and pC3 and no obvious correlation with the degree of cold-sensitive phenotype is apparent in this case. Since none of the regulatory elements of the rRNA promoters had been modified and no separate transcription start site between the 16S and the 23S rRNAs exists (45), the observed 16S rRNA deficiency can only be attributed to a reduced stability of those 16S rRNA molecules that are derived from mutant boxC operons.

To determine the *in vivo* stabilities of wild-type and boxC mutant rRNAs in more detail we measured the exact half-lives of the transcripts in exponentially growing cells. Total RNA was extracted at distinct time intervals after rifampicin addition (20–300 s) and rRNA precursor degradation was quantified by a primer extension reaction. A primer oligonucleotide complementary to the rRNA leader region (position L-38–L-56) was employed giving rise to cDNAs extending to the transcription start sites of rRNA promoters P1 and P2. With regard to the cold-sensitive phenotype, RNA turnover was analysed at two different temperatures, 30 and 37°C. Results after gel separation are summarised in Figure 6. Bands characteristic for transcription start at the P1 and P2 promoters can be seen. Most of the rRNA extracted is of plasmid origin. Note, however, that each promoter start is represented by more than one band due to leader sequence length heterogeneity of the different chromosomal rRNA operons. Although the absolute half-lives of pre-rRNAs initiated at the P1 and P2 promoters differ slightly, they follow the same tendency. For the wild-type transcript starting from promoter P2 we determined very short half-lives of $t_{½}$ = 69 and 144 s at 37 or 30°C, respectively. The pC1 mutant RNA is somewhat more stable with half-lives of $t_{½}$ = 84 and 201 s at the two different temperatures. The boxC mutations in pC2 and pC3 cause a remarkable enhancement in the lifetimes of the corresponding precursor transcripts (see Fig. 6A and B). Within the timescale of our experiment there is hardly any turnover of these molecules visible, indicating a $t_{½}$ significantly longer than 5 min. Since an oligonucleotide complementary to a sequence within the leader was employed for the analysis, the above experiment does not tell us whether the boxC mutations stabilise the isolated leader RNA after it had been cleaved off from the primary transcript or whether the precursor transcript with the leader still linked to the 16S rRNA is stabilised. This question could be answered by northern blot analysis, which revealed that the primer extension signals in Figure 6 represented precursor transcripts with the leader still attached to the 16S rRNA (see Fig. 7). For both wild-type and mutant cells the cleaved leader RNA alone is too short-lived to be detected by northern hybridisation. Obviously, the dramatic increase in lifetime of the precursor rRNA caused by the boxC mutations results from an impaired RNase III processing cut, which normally removes the leader RNA from the 16S rRNA transcript. This is not unexpected, since boxC represents the 5′-part of the RNase III processing stem formed by the sequence elements flanking the mature 16S rRNA. We therefore analysed the fate of rRNA precursors in cells which are defective in the gene for RNase III. Two

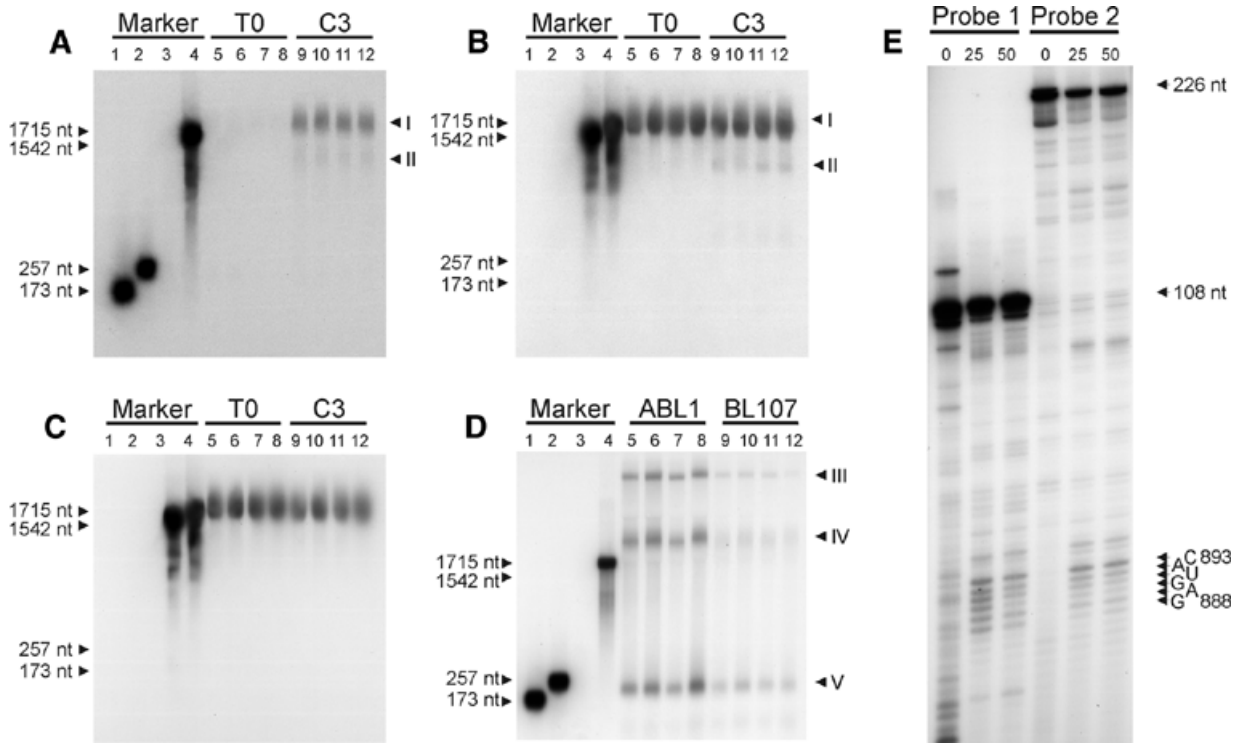

Figure 7. Northern and nuclease protection analysis of mutant rRNA transcripts. (**A**–**D**) RNA from the strains indicated above was analysed by northern hybridisation after rifampicin addition. The positions of the probes separated in lanes 1–4 are given in the margin (lane 1, leader only; lane 2, leader plus 84 nt of 16S rRNA; lane 3, 16S rRNA only; lane 4, leader plus complete 16S rRNA). Time after rifampicin addition: lanes 5 and 9, 20 s; lanes 6 and 10, 60 s; lanes 7 and 11, 150 s; lanes 8 and 12, 300 s. The following complementary oligonucleotide hybridisation probes were used: (A) and (D), leader region positions L-38–L-56; (B) 16S rRNA positions 866–883; (C) 16S rRNA positions 893–912. The different hybridisation products are indicated by Roman numerals I–V. Due to the low resolution of the gel system band I characterises products of the size of 16S rRNA and 16S rRNA plus the leader. Band II points to the newly identified product dependent on the boxC mutation. Band III represents the complete 30S precursor transcript. Band IV represents a similar product to I with both ends not processed by RNase III. Band V indicates the position of a truncated leader not processed by RNase III. (**E**) S1 nuclease protection analysis with 16S rDNA fragments, positions 838–945 (Probe 1) and 838–1053 (Probe 2). 0, 25 and 50 indicate no, 25 or 50 U S1, respectively. The 3′-end(s) of the transcript is indicated by arrows.

different RNase III$^-$ strains (ABL1 and BL107) were employed and the turnover of precursor rRNA after addition of rifampicin was determined as described above. Results presented in Figure 6C show that strains lacking RNase III accumulate a similar long-lived rRNA precursor to that observed in the boxC mutants. However, in contrast to boxC mutant strains that are able to express functional RNase III, the cleaved leader RNA is perfectly stable in strains lacking RNase III (see Fig. 7D, band V). This is a clear indication that one of the nucleases for which ABL1 and BL107 are defective must be involved in degradation of the cleaved leader. It is important to note that accumulation of precursor rRNAs in the boxC mutants and in the RNase III$^-$ strains does not mean that the 16S rRNA cannot be processed correctly. Correct processing of 16S rRNA is evident from the maxicell analysis and has generally been shown for RNase III$^-$ strains. Interestingly, the same processing cut that is performed by RNase III can be observed in a RNase III-defective strain, however, to a much weaker extent (data not shown). This observation is consistent with the notion that RNase III is dispensable in *E.coli*.

The observation that inhibition of the RNase III processing step does not prevent rRNA transcripts derived from mutant boxC operons entering the pool of active ribosomal particles could be corroborated by two different experiments. First, combination of the boxC mutation with a C→U base change at position 1192 within the 16S rRNA structural gene conferring spectinomycin resistance (pC3-Spec) allows determination of the origin of mature 16S rRNA from different ribosomal pools. The signal characteristic for the spectinomycin resistance mutation can be quantified by primer extension analysis of rRNA from different ribosomal fractions and thus the amount of transcript originating from mutant operons can be determined (14,42). It turned out from a series of such primer extension analyses that the spectinomycin resistance mutation can be found in all cellular ribosome fractions, including translationally active polysomes (Table 1). Second, plasmids with the boxC mutation could be transformed in strain TA554 (26), in which all chromosomal rRNA operons have been inactivated (kindly provided by C. Squires). Such transformants are viable in the absence of any other wild-type rRNA operon. We conclude from these experiments that the disturbance in RNase III processing by base changes in the boxC region do not prevent formation of 30S ribosomes which are fully active and functionally indistinguishable from wild-type subunits.

Next we wished to determine whether effects other than impairment of the initial RNase III processing cut might be responsible for the cold-sensitive phenotype conferred by the boxC mutations. For this reason we determined in more detail if mature rRNAs were correctly processed or if aberrant rRNA

Table 1. Amounts of mutant rRNA in different ribosomal populations

	pT0-Spec			pC1-Spec			pC2-Spec			pC3-Spec		
	30S	70S	P	30S	70S	P	30S	70S	P	30S	70S	P
Chromosome	17	17	17	26	26	26	21	23	26	23	24	23
Plasmid	83	83	83	74	74	74	79	77	76	77	76	77

The amounts of plasmid versus chromosome encoded rRNAs are given as percentages. 30S, 70S and P (polysomes) denote the respective fractions from sucrose gradients. Wild-type and the different mutant strains are denoted in the top row.

intermediates occurred. Apart from the existence of a small amount of precursor rRNA no differences at the 5′-ends of processed 16S rRNAs could be detected between wild-type and boxC mutants by primer extension analysis of rRNAs from exponentially growing cells (data not shown). In addition, major differences at the 3′-end can be ruled out by length comparison of the mature rRNAs. However, by northern analysis of RNA from wild-type and pC3 mutants after rifampicin addition we detected the existence of an aberrant ~1220 nt processing/degradation product. This aberrant product occurred exclusively in the mutant. It hybridised to probes complementary to the rRNA leader as well as to sequences complementary to the first 880 nt of the mature 16S rRNA (see Fig. 7A and B, band II). The exact 3′-terminus of the processing/degradation intermediate was characterised by S1 nuclease and primer extension sequencing to map at 16S rRNA positions 888–893 (Fig. 7E). Since this product is completely absent in strains lacking RNase III we conclude that the new product does not depend on accumulation of unprocessed 16S rRNA precursor. We rather believe that the newly characterised degradation product is the consequence of a structural deformation induced by the mutant leader that is transmitted to the 16S sequence where it gives rise to an aberrant degradation process. With the 1220 nt rRNA fragment we have characterised a first intermediate of this degradative pathway. It should be noted that the 3′-end of the intermediate is localised in the vicinity of 16S rRNA helix 2, adjacent to helices 19 and 27. These three helices are very close to the central pseudoknot, which is a crucial structural element for the correct biogenesis pathway of 30S subunits.

In conclusion, the results reported in this manuscript support the view that conserved sequences of the bacterial rRNA leader participate in correct structure formation and maturation of the small subunit rRNA. Results are also consistent with a straightforward mechanism according to which the leader, through its higher order structure, makes transient contacts with distinct sites of the 16S rRNA. These structural intermediates facilitate and guide the correct folding and maturation processes. In the absence of the transient leader contacts the normal folding path is changed, which, dependent on the available activation energy, may result in aberrant structures that are subject to enhanced turnover. It is also feasible that 30S particles that are incorrectly folded or incompletely assembled due to base changes in the leader are rapidly degraded as a kind of quality control step.

SUPPLEMENTARY MATERIAL

Supplementary Material is available at NAR Online.

ACKNOWLEDGEMENTS

We would like to thank J. Eberle for construction of the boxC mutations. We are greatly indebted to C. Squires for providing us with strain TA554. T7 polymerase was a kind gift of B. Esters. The work was supported by the Deutsche Forschungsgemeinschaft. J.S. is the recipient of a Düsseldorf Entrepreneurs Foundation fellowship.

REFERENCES

1. Brimacombe,R. (2000) The bacterial ribosome at atomic resolution. *Struct. Fold Des.*, **8**, 195–200.
2. Wimberly,B.T., Brodersen,D.E., Clemans,W.M., Morgan-Warren,R.J., Carter,A.P., Vonheln,C., Hartsch,T. and Ramakrishnan,V. (2000) Structure of the 30S ribosomal subunit. *Nature*, **407**, 327–339.
3. Cate,J.H., Yusupov,M.M., Yusupova,G.Z., Earnest,T.N. and Noller,H.F. (1999) X-ray crystal structures of 70S ribosome functional complexes. *Science*, **285**, 2095–2104.
4. Porse,B.T. and Garrett,R.A. (1999) Ribosomal mechanics, antibiotics and GTP hydrolysis. *Cell*, **97**, 423–426.
5. Cech,T.R. (2000) The ribosome is a ribozyme. *Science*, **289**, 878–879.
6. Nissen,P., Hansen,J., Ban,N., Moore,P.B. and Steitz,T.A. (2000) The structural basis of ribosome activity in peptide bond synthesis. *Science*, **289**, 920–930.
7. Rodnina,M.V., Stark,H., Savelsbergh,A., Wieden,H.J., Mohr,D., Matassova,N.B., Peske,F., Daviter,T., Gualerzi,C.O. and Wintermeyer,W. (2000) GTPases mechanisms and functions of translation factors on the ribosome. *Biol. Chem.*, **381**, 377–387.
8. Wagner,R. (1994) The regulation of ribosomal RNA synthesis and bacterial cell growth. *Arch. Microbiol.*, **160**, 100–109.
9. Gourse,R.L., Gaal,T., Bartlett,M.S., Appleman,J.A. and Ross,W. (1996) rRNA transcription and growth rate-dependent regulation of ribosome synthesis in *Escherichia coli*. *Annu. Rev. Microbiol.*, **50**, 645–677.
10. Lindahl,L. and Zengel,J.M. (1986) Ribosomal genes in *Escherichia coli*. *Annu. Rev. Genet.*, **20**, 297–326.
11. King,T.C., Sirdeskmukh,R. and Schlessinger,D. (1986) Nucleolytic processing of ribonucleic acids transcripts in procaryotes. *Microbiol. Rev.*, **50**, 428–451.
12. Srivastava,A.K. and Schlessinger,D. (1990) Mechanism and regulation of bacterial ribosomal RNA processing. *Annu. Rev. Microbiol.*, **44**, 105–129.
13. Theißen,G., Thelen,L. and Wagner,R. (1993) Some base substitutions in the leader of an *E. coli* ribosomal RNA operon affect the structure and function of ribosomes—evidence for a transient molecular scaffold-like function of the rRNA leader. *J. Mol. Biol.*, **233**, 203–218.
14. Pardon,B., Thelen,L. and Wagner,R. (1994) The *Escherichia coli* ribosomal RNA leader: a structural and functional investigation. *Biol. Chem. Hoppe Seyler*, **375**, 11–20.
15. Pardon,B. and Wagner,R. (1995) The *Escherichia coli* ribosomal RNA leader *nut* region interacts specifically with mature 16S RNA. *Nucleic Acids Res.*, **23**, 932–941.
16. Besançon,W. and Wagner,R. (1999) Characterization of transient RNA–RNA interactions important for the facilitated structure formation of bacterial ribosomal 16S RNA. *Nucleic Acids Res.*, **22**, 4353–4362.
17. Liiv,A., Tenson,T., Margus,T. and Remme,J. (1998) Multiple functions of the transcribed spacers in ribosomal RNA operons. *Biol. Chem.*, **379**, 783–793.

18. Hughes,J.M.X. (1996) Functional base-pairing interaction between highly conserved elements of U3 small nucleolar RNA and the small ribosomal subunit RNA. *J. Mol. Biol.*, **259**, 645–654.
19. Steitz,J.A. and Tycowski,K.T. (1995) Small RNA chaperones for ribosome biogenesis. *Science*, **270**, 1626–1627.
20. Li,S.C., Squires,C.L. and Squires,C. (1984) Antitermination of *E. coli* rRNA transcription is caused by a control region segment containing lambda *nut*-like sequences. *Cell*, **38**, 851–860.
21. Dennis,P.P., Russell,A.G. and De Sa,M.M. (1997) Formation of the 5′ end pseudoknot in small subunit ribosomal RNA: involvement of U3-like sequences. *RNA*, **3**, 337–343.
22. Boyer,H.W. and Roulland-Dussoix,D. (1969) A complementation analysis of the restriction and modification of DNA in *Escherichia coli*. *J. Mol. Biol.*, **41**, 459–472.
23. Sancar,A., Hack,A.M. and Rupp,W.D. (1979) Simple method for identification of plasmid-coded proteins. *J. Bacteriol.*, **137**, 692–693.
24. Studier,F.W. (1975) Genetic mapping of a mutation that causes ribonuclease III deficiency in *Escherichia coli*. *J. Bacteriol.*, **124**, 307–316.
25. Robertson,H.D., Pelle,E.G. and McLain,D.K. (1980) RNA processing in an *Escherichia coli* strain deficient in both RNase P and RNase III. In Söll,D., Abelson,J. and Schimmel,P. (eds) *Transfer RNA*, *Biological Aspects*. Cold Spring Harbor Laboratory Press, Cold Spring Harbor, NY, pp. 107–122.
26. Asai,T., Zaporojets,D., Squires,C. and Squires,C.L. (1999) An *Escherichia coli* strain with all chromosomal rRNA operons inactivated: complete exchange of rRNA genes between bacteria. *Proc. Natl Acad. Sci. USA*, **96**, 1971–1976.
27. Bolivar,F., Rodriguez,R.L., Green,P.J., Betlach,M., Heyneker,H.L., Boyer,H.W., Crosa,J. and Falkow,S. (1977) Construction and characterization of new cloning vehicles. II. A multipurpose cloning system. *Gene*, **2**, 95–113.
28. Brosius,J., Dull,T.J., Sleeter,D.D. and Noller,H.F. (1981) Gene organization and primary structure of a ribosomal RNA operon from *E. coli*. *J. Mol. Biol.*, **148**, 107–125.
29. Theißen,G., Eberle,J., Zacharias,M., Tobias,L. and Wagner,R. (1990) The t_L structure within the leader region of *E. coli* ribosomal RNA operons has post-transcriptional functions. *Nucleic Acids Res.*, **18**, 3893–3901.
30. Triman,K., Becker,E., Dammel,C., Katz,J., Mori,H., Douthwaite,S., Yapijakis,C., Yoast,S. and Noller,H.F. (1989) Isolation of temperature-sensitive mutants of 16S rRNA in *Escherichia coli*. *J. Mol. Biol.*, **209**, 645–653.
31. Sambrook,J., Fritsch,E.F. and Maniatis,T. (1989) *Molecular Cloning: A Laboratory Manual*, 2nd Edn. Cold Spring Harbor Laboratory Press, Cold Spring Harbor, NY.
32. Rosenbaum,V. and Riesner,D. (1987) Temperature-gradient gelelectrophoresis: thermodynamic analysis of nucleic acids and proteins in purified form and in cellular extracts. *Biophys. Chem.*, **26**, 235–246.
33. Ehresmann,C., Baudin,F., Mougel,M., Romby,P., Ebel,J.P. and Ehresmann,B. (1987) Probing the structure of RNAs in solution. *Nucleic Acids Res.*, **22**, 9109–9128.
34. Göringer,H.U., Bertram,S. and Wagner,R., (1984) The effect of tRNA binding on the structure of 5S RNA in *E. coli*. A chemical modification study. *J. Biol. Chem.*, **259**, 491–496.
35. Stern,S., Moazed,D. and Noller,H.F. (1988) Structural analysis of RNA using chemical and enzymatic probing monitored by primer extension. *Methods Enzymol.*, **164**, 481–489.
36. Stark,M.J.R., Gourse,R.L. and Dahlberg,A.E., (1982) Site-directed mutagenesis of ribosomal RNA. Analysis of ribosomal RNA deletion mutants using maxicells. *J. Mol. Biol.*, **159**, 417–439.
37. Szymkowiak,C. and Wagner,R. (1987) Effects of deletions in the spacer region of the *rrnB* operon on the transcription of the large ribosomal RNAs from *Escherichia coli*. *Mol. Microbiol.*, **1**, 327–334.
38. Sarmientos,P. and Cashel,M. (1983) Carbon starvation and growth rate-dependent regulation of the *Escherichia coli* ribosomal RNA promoters: differential control of dual promoters. *Proc. Natl Acad. Sci. USA*, **80**, 7010–7013.
39. Afflerbach,H., Schröder,O. and Wagner,R. (1998) Effects of the *Escherichia coli* DNA-binding protein H-NS on rRNA synthesis *in vivo*. *Mol. Microbiol.*, **28**, 641–654.
40. Theißen,G., Behrens,S.E. and Wagner,R. (1990) Functional importance of the *E. coli* ribosomal RNA leader box A sequence for post-transcriptional events. *Mol. Microbiol.*, **4**, 1667–1678.
41. Godson,G.N. and Sinsheimer,R.L. (1967) Use of brij lysis as a general method to prepare polyribosomes from *Escherichia coli*. *Biochim. Biophys. Acta*, **149**, 489–495.
42. Sigmund,C.D., Ettayebi,M., Borden,A. and Morgan,E.A. (1988) Antibiotic resistance mutations in rRNA genes of *Escherichia coli*. *Methods Enzymol.*, **164**, 673–690.
43. Göringer,H.U., Szymkowiak,C. and Wagner,R. (1984) 5S RNA A- and B-conformers: characterisation by enzymatic and chemical methods. *Eur. J. Biochem.*, **114**, 25–34.
44. Brimacombe,R., Atmadja,J., Stiege,W. and Schüler,D. (1988) A detailed model of the three-dimensional structure of *Escherichia coli* 16S ribosomal RNA *in situ* in the 30S subunit. *J. Mol. Biol.*, **199**, 115–136.
45. Zacharias,M. and Wagner,R. (1989) Functional characterization of a putative internal promoter sequence within the *E. coli rrnB* operon. *Mol. Microbiol.*, **3**, 405–410.